

# Microstructural evolution in sol–gel derived P<sub>2</sub>O<sub>5</sub>-doped cordierite powders

Sen Mei, Juan Yang, J.M.F. Ferreira \*

*Department of Ceramics and Glass Engineering, UIMC, University of Aveiro, 3810-193 Aveiro, Portugal*

Received 5 August 1999; received in revised form 9 February 2000; accepted 14 February 2000

## Abstract

The purpose of this paper is to analyse the effect of various amounts of P<sub>2</sub>O<sub>5</sub> additive on the microstructural evolution of cordierite. In this research work, cordierite powders were prepared by sol–gel processing. The phase and microstructural evolution of the powders were characterised by DTA, XRD and SEM. The P<sub>2</sub>O<sub>5</sub> additive was found to promote the  $\mu$ -cordierite to  $\alpha$ -cordierite transition at low concentrations, while a non-steady effect was shown for higher concentrations. The effect of P<sub>2</sub>O<sub>5</sub> on the activation of cordierite can be attributed to the nucleation of P<sub>2</sub>O<sub>5</sub> and the formation of mullite and  $x$ MgO–P<sub>2</sub>O<sub>5</sub> based compounds ( $x = 3, 2, 1$ ). © 2000 Elsevier Science Ltd. All rights reserved.

*Keywords:* Cordierite; Microstructure; P<sub>2</sub>O<sub>5</sub>; Powders; Sol–gel processes

## 1. Introduction

Cordierite and cordierite-based glass-ceramics have attracted interest in recent years because they have excellent dielectric properties ( $\sim 5$  at 1 MHz, with low dielectric loss). However, cordierite alone is difficult to sinter because of the narrow temperature range, within 25°C of its incongruent melting point (1445°C) and has relatively poor mechanical properties, which have prevented its widespread application.<sup>1</sup> Therefore, composite materials based on cordierite and glass, have been proposed as suitable candidates for microelectronics applications because they can be co-fired with copper at low temperatures (below 1000°C), and can match silicon in thermal expansion characteristics ( $1\text{--}2 \times 10^{-6}/\text{K}$  from 25 to 1000°C).<sup>2–4</sup>

In the conventional preparation process of cordierite powders, some nucleating agents, such as P<sub>2</sub>O<sub>5</sub>, B<sub>2</sub>O<sub>3</sub> or TiO<sub>2</sub>, are usually added to stoichiometric cordierite to control its crystallisation and decrease sintering temperatures.<sup>5–8</sup> The addition of nucleating agents also plays an important role in modifying the phase transformation of cordierite precursors. Knickerbocker et al.<sup>9</sup> found that even a small amount of B<sub>2</sub>O<sub>3</sub> and P<sub>2</sub>O<sub>5</sub>

was effective in controlling the crystallisation of cordierite glasses and promoting the  $\mu$ -cordierite to  $\alpha$ -cordierite transition. Rudolph et al.<sup>10</sup> studied the effect of P<sub>2</sub>O<sub>5</sub> on the activation energies for crystallisation of cordierite glasses. They observed apparent activation energy values in the range of 470–500 kJ/mol either in static or dynamic tests, although the polymorph formed is not referred to. Crystallisation behaviour in the non-stoichiometric compositions of the system MgO–Al<sub>2</sub>O<sub>3</sub>–SiO<sub>2</sub> was also studied by Amista et al.<sup>11</sup> They found that the nature of the excess component actually changes the stability ranges of  $\mu$ -cordierite and  $\alpha$ -cordierite. The calculated activation energies for the crystallisation of  $\mu$ -cordierite and for the transformation of  $\mu$ - to  $\alpha$ -cordierite by the non-isothermal method were about 356 and 565 kJ/mol, respectively. However, there are few reports on the mechanism of the influence of P<sub>2</sub>O<sub>5</sub> and B<sub>2</sub>O<sub>3</sub> additives on the phase transition.

Recently, pure and crystalline cordierite powders were prepared by the sol–gel method using metal alkoxides.<sup>12</sup> The preparation of cordierite-based glass-ceramics in the ternary system by so-called sol–gel techniques has been extensively used.<sup>13,14</sup> Sol–gel processing can be used to synthesise multi-component ceramics with high chemical uniformity at lower temperatures and without any sintering aid compared with those required in conventional processes.

\* Corresponding author. Fax: +351-234-425-300.

E-mail address: jmf@cv.ua.pt (J.M.F. Ferreira).

In the present investigation, stoichiometric cordierite powders and  $P_2O_5$ -doped cordierite powders were prepared by sol–gel processing. The purpose of this research is to analyse the effect of  $P_2O_5$  alone on the microstructural evolution and transformation of  $\mu$ -cordierite to  $\alpha$ -cordierite. The variation of the crystallisation behaviour of pure stoichiometric and  $P_2O_5$ -doped cordierite powders was also investigated.

## 2. Experimental procedure

### 2.1. Powder preparation

Cordierite and  $P_2O_5$ -doped cordierite powders were synthesised from tetraethyl orthosilicate (TEOS, Fluka Chemie AG, CH-9470, Buchs),  $Al(NO_3)_3 \cdot 9H_2O$  (Merck KgaA, Germany) and  $Mg(NO_3)_2 \cdot 6H_2O$  (Merck KgaA, Germany). TEOS,  $Al(NO_3)_3 \cdot 9H_2O$  and  $Mg(NO_3)_2 \cdot 6H_2O$  were dissolved under vigorous stirring in ethanol and then hydrolysed by mixing with distilled water (molar ratio  $H_2O/TEOS=20$ ) catalysed with  $HNO_3$ . Orthophosphoric acid (BDH Chemicals Ltd Poole, UK) was then added in different proportions according to  $P_2O_5/(P_2O_5 + \text{cordierite})$  weight ratios of 1.77, 3.47, 6.70, 9.74, 12.57 and 15.24%. These samples will hereafter be referred to as  $S_0$ – $S_6$ , successively. The resulting gels were held at room temperature for 8 h and then were dried in an oven at 60 and 120°C for 1 day at each temperature.

### 2.2. Analytical methods

For XRD analysis, the as-prepared gel powders were ground and then heated at 5°C/min from room temperature up to 300°C, then at 3°C/min up to 500°C to burn out organic matter, followed by a heating rate of 10°C/min up to different desired temperatures with various holding times. The crystalline phases were identified by using an X-ray diffractometer (D/Max-C, Rigaku, Japan) scanning from 5 to 70° with a scanning speed of 3°/min. The degree of conversion from  $\mu \rightarrow \alpha$ -cordierite,  $f$ , was determined by using the following equation:<sup>15</sup>

$$f = \frac{1}{1 + K^* \frac{I_{\mu(101)}}{I_{\alpha(110)}}} \quad (1)$$

where  $I_{\mu(101)}$  is the integral intensity corresponding to the (101) peak for  $\mu$ -cordierite and  $I_{\alpha(110)}$  is the integral intensity corresponding to the (110) peak for  $\alpha$ -cordierite, and  $K$  is a constant close to unit ( $K \approx 1$ ).<sup>15</sup> The microstructure of the samples was observed by scanning electron microscopy (SEM) (Hitachi-4100, Japan). For a better comprehension of the crystallisation in this system, differential thermal analysis (DTA) (in-house constructed) was performed on the sol–gel derived powders,

having average particle sizes of about 5  $\mu$ , including stoichiometric cordierite powder and the  $P_2O_5$ -doped powders. Samples were heated in air up to 1200°C at different rates of 3, 5, 10, 15, 20, 40°C/min with an alumina reference for calculating activation energies of the  $\mu$ -cordierite to  $\alpha$ -cordierite transition. Particle sizes of gel powders used for DTA measurements were determined by Coulter LS230 instrument (Coulter Electronics Limited, England). Assuming that the kinetics of the crystallisation process is described by the equation of Kissinger,<sup>16</sup> the activation energies are calculated via the expression:

$$\ln(\phi/T_p^2) = E_{ck}/RT_p + \text{const} \quad (2)$$

where  $\phi$  is the DTA heating rate,  $T_p$  is the crystallisation peak temperature;  $E_{ck}$  is the activation energy for crystallisation estimated by the Kissinger method; and  $R$  is the gas constant.

## 3. Results

### 3.1. XRD analysis

The phase evolution of polymeric cordierite gel after heat treatment at 950, 1100 and 1300°C is listed in Table 1. For the samples heat-treated at 950°C for 2 h, strong  $\mu$ -cordierite peaks together with traces of mullite and spinel phases could be observed in the stoichiometric sample  $S_0$ . With increasing  $P_2O_5$  additive,  $\mu$ -cordierite,  $\alpha$ -cordierite, mullite, farringtonite and spinel all appear in the  $P_2O_5$ -doped samples from  $S_1$  to  $S_3$ , whereas only  $\mu$ -cordierite, mullite, magnesium pyrophosphate are present in  $S_4$  to  $S_6$ . Therefore, one can say that a certain amount of  $P_2O_5$  additive promotes the  $\mu$ - to  $\alpha$ -cordierite transition, while it also leads to the formation of undesired phases such as spinel and mullite.

For the samples heat-treated at 1100°C for 2 h, it was found that  $\mu$ -cordierite was the main polymorph to be formed, together with traces of mullite and  $\alpha$ -cordierite in the stoichiometric sample. However, for  $P_2O_5$ -doped samples (from  $S_1$  to  $S_3$ ), the intensity ratio  $I_{\alpha(110)}/I_{\mu(101)}$  is much higher than that of the stoichiometric sample,  $S_0$ . The intensity ratio abruptly decreases for  $S_4$  and becomes almost unity for  $S_5$ , decreasing again for  $S_6$  to a level similar to  $S_4$ . Besides the intensity ratio, no other significant differences could be observed between the XRD results of  $S_0$  and those of samples from  $S_4$  to  $S_6$ , except an increasing amount of mullite appearing in the  $P_2O_5$ -doped samples.

Farringtonite ( $3MgO \cdot P_2O_5$ ) is detected in the samples from  $S_1$  to  $S_3$  heat-treated for 2h, whereas magnesium pyrophosphate ( $2MgO \cdot P_2O_5$ ) is detected in  $S_4$ – $S_6$ . Some additional small peaks are also detected, which can be ascribed to presence of spinel phase,  $MgO \cdot Al_2O_3$ .

Table 1  
Crystalline phases formed in the S series samples heat-treated at different temperatures for two different holding times

| Samples        | 950°C/2 h                    | 1100°C/2 h                 | $I_{\alpha(110)}/I_{\mu(101)}$ | 1100°C/4 h                 | $I_{\alpha(110)}/I_{\mu(101)}$ | 1300°C/2 h       |
|----------------|------------------------------|----------------------------|--------------------------------|----------------------------|--------------------------------|------------------|
| S <sub>0</sub> | $\mu^b + M + S$              | $\mu + \alpha + M + S^f$   | 0.3                            | $\mu + \alpha + S$         | 13.4                           | $\alpha^a$       |
| S <sub>1</sub> | $\mu + \alpha + M + F^c + S$ | $\mu + \alpha + M + F + S$ | 14.3                           | $\mu + \alpha + S$         | 39.3                           | $\alpha$         |
| S <sub>2</sub> | $\mu + \alpha + M + F + S$   | $\mu + \alpha + M + F + S$ | 12.5                           | $\mu + \alpha + S$         | 18.9                           | $\alpha$         |
| S <sub>3</sub> | $\mu + \alpha + M + F + S$   | $\mu + \alpha + M + F + S$ | 7.0                            | $\mu + \alpha + M + F + S$ | 0.8                            | $\alpha + M$     |
| S <sub>4</sub> | $\mu + M + P^d$              | $\mu + \alpha + M + P$     | 0.1                            | $\mu + M + P$              | 0                              | $\alpha + M + P$ |
| S <sub>5</sub> | $\mu + M^e + P$              | $\mu + \alpha + M + P$     | 1.1                            | $\mu + \alpha + M + P$     | 0.2                            | $\alpha + M + P$ |
| S <sub>6</sub> | $\mu + M + P$                | $\mu + \alpha + M + P$     | 0.1                            | $\mu + \alpha + M + P$     | 0.1                            | $\alpha + M + P$ |

<sup>a</sup>  $\alpha$ :  $\alpha$ -cordierite.

<sup>b</sup>  $\mu$ :  $\mu$ -cordierite.

<sup>c</sup> F: Farringtonite (3MgO·P<sub>2</sub>O<sub>5</sub>).

<sup>d</sup> P: Magnesium pyrophosphate (2MgO·P<sub>2</sub>O<sub>5</sub>).

<sup>e</sup> M: Mullite (3Al<sub>2</sub>O<sub>3</sub>·2SiO<sub>2</sub>).

<sup>f</sup> S: Spinel (MgAl<sub>2</sub>O<sub>4</sub>).

With increasing heat-treatment time at 1100°C, the intensity ratio  $I_{\alpha(110)}/I_{\mu(101)}$  increased at low P<sub>2</sub>O<sub>5</sub> additive concentrations from S<sub>0</sub> to S<sub>2</sub>, while it decreased for S<sub>3</sub> and S<sub>4</sub>. The heat-treatment time did not promote significant changes in the phases present for higher P<sub>2</sub>O<sub>5</sub> contents. Farringtonite is detected only in S<sub>3</sub>.

With the temperature increased to 1300°C,  $\mu$ -cordierite has been transformed into  $\alpha$ -cordierite in all samples. Moreover, magnesium pyrophosphate is still detected at higher P<sub>2</sub>O<sub>5</sub> additive concentrations from S<sub>4</sub> to S<sub>6</sub>.

Due to overlapping, identified peaks were isolated by peak deconvolution and the degree of conversion from  $\mu$ -cordierite to  $\alpha$ -cordierite was calculated according to Eq. (1). The degree of conversion from  $\mu \rightarrow \alpha$ -cordierite for different P<sub>2</sub>O<sub>5</sub> additive concentrations in the samples heat-treated at 1100°C for 4 h is shown in Fig. 1. S<sub>1</sub> has a higher  $f$  value than the stoichiometric sample, S<sub>0</sub>. This indicates that P<sub>2</sub>O<sub>5</sub> additive slightly favours the transition from  $\mu$ -cordierite to  $\alpha$ -cordierite at low concentrations.

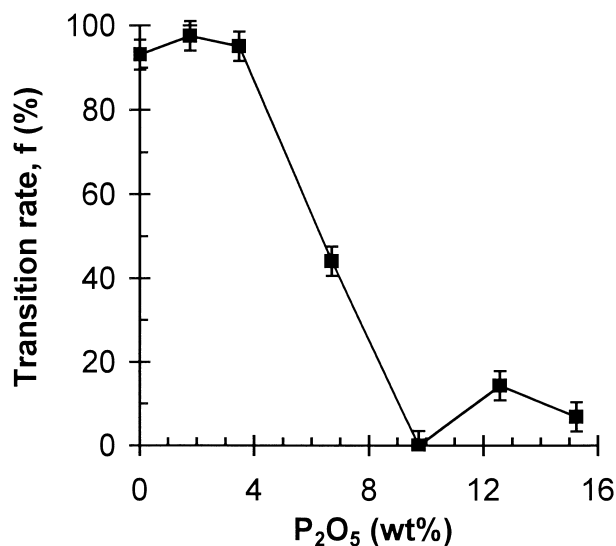


Fig. 1. The degree of conversion of S series samples heat treated at 1100°C for 4 h.

Similar  $f$  values can be observed in the samples S<sub>0</sub> and S<sub>2</sub>. With the P<sub>2</sub>O<sub>5</sub> additive concentrations further increasing, the degree of conversion is lower than that of S<sub>0</sub>, although an increasing value can be observed in the sample S<sub>5</sub>. It can be concluded that higher additive concentrations play an inhibitory role in the MgO–Al<sub>2</sub>O<sub>3</sub>–SiO<sub>2</sub> system.

### 3.2. Differential thermal analysis (DTA)

The Kissinger plots according to Eq. (2) are shown in Fig. 2. Based on these data, the calculated activation energies for the  $\mu$ -cordierite to  $\alpha$ -cordierite transition are presented in Table 2. It can be seen that the stoichiometric cordierite shows an activation energy value of 235 kJ/mol, which is about half of the values already reported for glassy cordierite powders prepared by melting.<sup>10,11</sup> From Table 2, it can also be noticed that the activation energy decreases for the sample containing the lowest amount of P<sub>2</sub>O<sub>5</sub> additive 1.77 wt% (S<sub>1</sub>) and then increases as the P<sub>2</sub>O<sub>5</sub> additive concentration increases up to 9.74 wt% (S<sub>4</sub>). The activation energies for the samples from S<sub>1</sub> to S<sub>4</sub> are 109, 276, 661, 701 kJ/mol, respectively. However, further additions of P<sub>2</sub>O<sub>5</sub> cause a decrease of the activation energy to 303 kJ/mol for S<sub>5</sub>, followed by an increase to 425 kJ/mol for S<sub>6</sub>. Therefore, P<sub>2</sub>O<sub>5</sub> additive promotes the  $\mu$ -cordierite to  $\alpha$ -cordierite transition up to concentrations of about 2 wt%, while a non-steady inhibitory effect is showed for higher concentrations.

### 3.3. Microstructural analysis by SEM

The morphology of powders heat-treated for 2 h at 950, 1100 and 1300°C is shown in Fig. 3. At 950°C there is no remarkable evidence that  $\mu$ -cordierite appears in S<sub>0</sub> (Fig. 3a), whereas it appears in S<sub>1</sub> (Fig. 3b). The dendritic morphology is characteristic of  $\mu$ -cordierite.<sup>17</sup> As the concentration of P<sub>2</sub>O<sub>5</sub> increases to 15.24 wt%

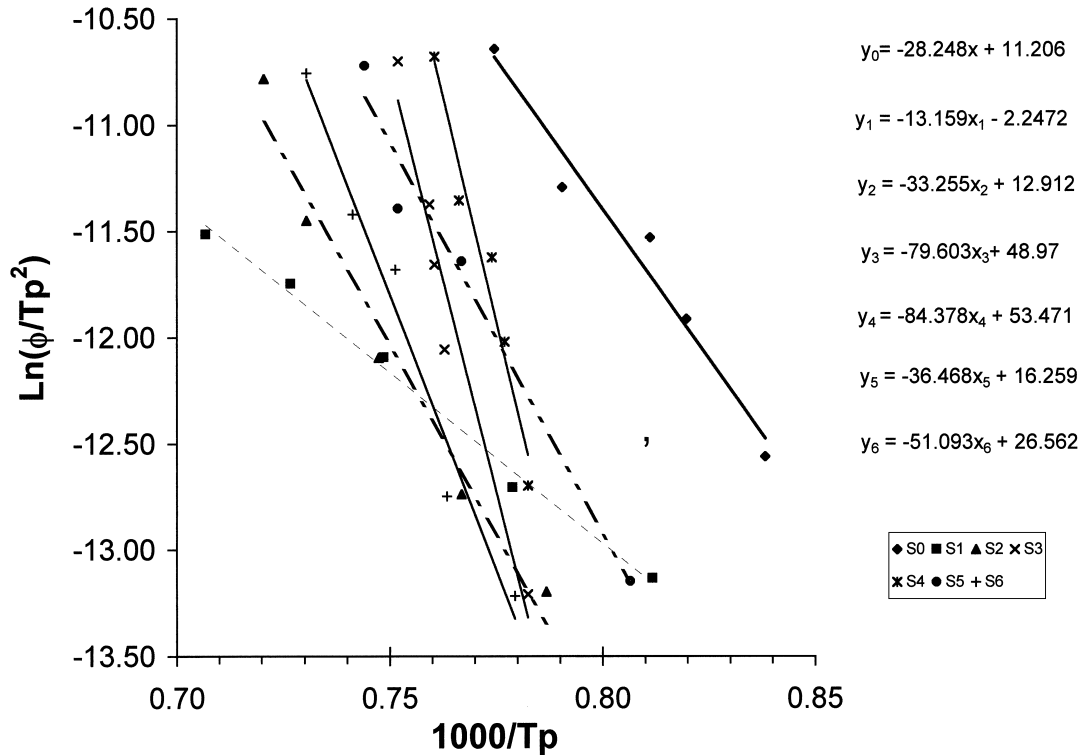


Fig. 2. The Kissinger plots for the S series samples.

Table 2  
The calculated activation energies ( $E_{ck}$ ) of S series samples

| Sample                              | S <sub>0</sub> | S <sub>1</sub> | S <sub>2</sub> | S <sub>3</sub> | S <sub>4</sub> | S <sub>5</sub> | S <sub>6</sub> |
|-------------------------------------|----------------|----------------|----------------|----------------|----------------|----------------|----------------|
| P <sub>2</sub> O <sub>5</sub> (wt%) | 0.00           | 1.77           | 3.47           | 6.70           | 9.74           | 12.57          | 15.24          |
| $E_{ck}$ (kJ/mol)                   | 235            | 109            | 276            | 661            | 701            | 303            | 425            |

(S<sub>6</sub>), only a few  $\mu$ -cordierite dendrites can be observed (Fig. 3c). Obviously, the addition of low-level of P<sub>2</sub>O<sub>5</sub> favours the formation of  $\mu$ -cordierite at the lower temperature, whereas higher additive concentrations delay the occurrence of  $\mu$ -cordierite. After heat-treatment for 2 h at 1100°C,  $\alpha$ -cordierite and  $\mu$ -cordierite appear in S<sub>1</sub> simultaneously (Fig. 3d and e), particles with cellular morphology appear, which were regarded as  $\alpha$ -cordierite.<sup>17</sup> This indicates that the transition  $\mu \rightarrow \alpha$ -cordierite occurs at about 1100°C as confirmed by the XRD results. At 1300°C, only  $\alpha$ -cordierite can be observed and no  $\mu$ -cordierite is present in S<sub>1</sub> (Fig. 3f).

#### 4. Discussion

DTA results show that the activation energy (235 kJ/mol) of  $\mu \rightarrow \alpha$ -cordierite transition for the stoichiometric cordierite powders is only about half of the values already reported for glassy cordierite powders prepared by melting.<sup>10,11</sup> This suggests that the powders prepared

by sol-gel processing should be more homogeneous than those obtained by melting, in which phase separation is likely to occur on cooling.<sup>11</sup> The small particle sizes of powders obtained by sol-gel method also favours the surface nucleation and crystallisation, lowering the activation energies for these processes.<sup>18</sup> However, the activation energies for the  $\mu \rightarrow \alpha$ -cordierite transformation are strongly affected by the presence and the amount of P<sub>2</sub>O<sub>5</sub> additive. Furthermore, the degree of  $\mu \rightarrow \alpha$ -cordierite transformation and the microstructure of the powders also depend on the temperature and time of heat-treatment. These factors will be discussed below.

The results presented show that at lower P<sub>2</sub>O<sub>5</sub> concentrations, the additive promotes the  $\mu \rightarrow \alpha$ -cordierite phase transition. This is according to other earlier reports.<sup>10,11</sup> The promoting effect is thought to be associated with the heterogeneous nucleating role played by P<sub>2</sub>O<sub>5</sub>.<sup>19</sup> However, a radically different explanation involving immiscibility of metastable liquid has also been thought as a possible cause of very fine segregation and fine-structured crystallisation.<sup>5</sup> Therefore, the mechanism still remains unclear and controversial. For higher additive concentrations, the P<sub>2</sub>O<sub>5</sub> starts to play an inhibitory effect and the activation energy for the  $\mu \rightarrow \alpha$ -cordierite transformation increases but in a non-steady way, as shown in Table 2. Such evolution can be attributed to the formation of farringtonite at intermediate P<sub>2</sub>O<sub>5</sub> concentrations (S<sub>2</sub> and S<sub>3</sub>) and

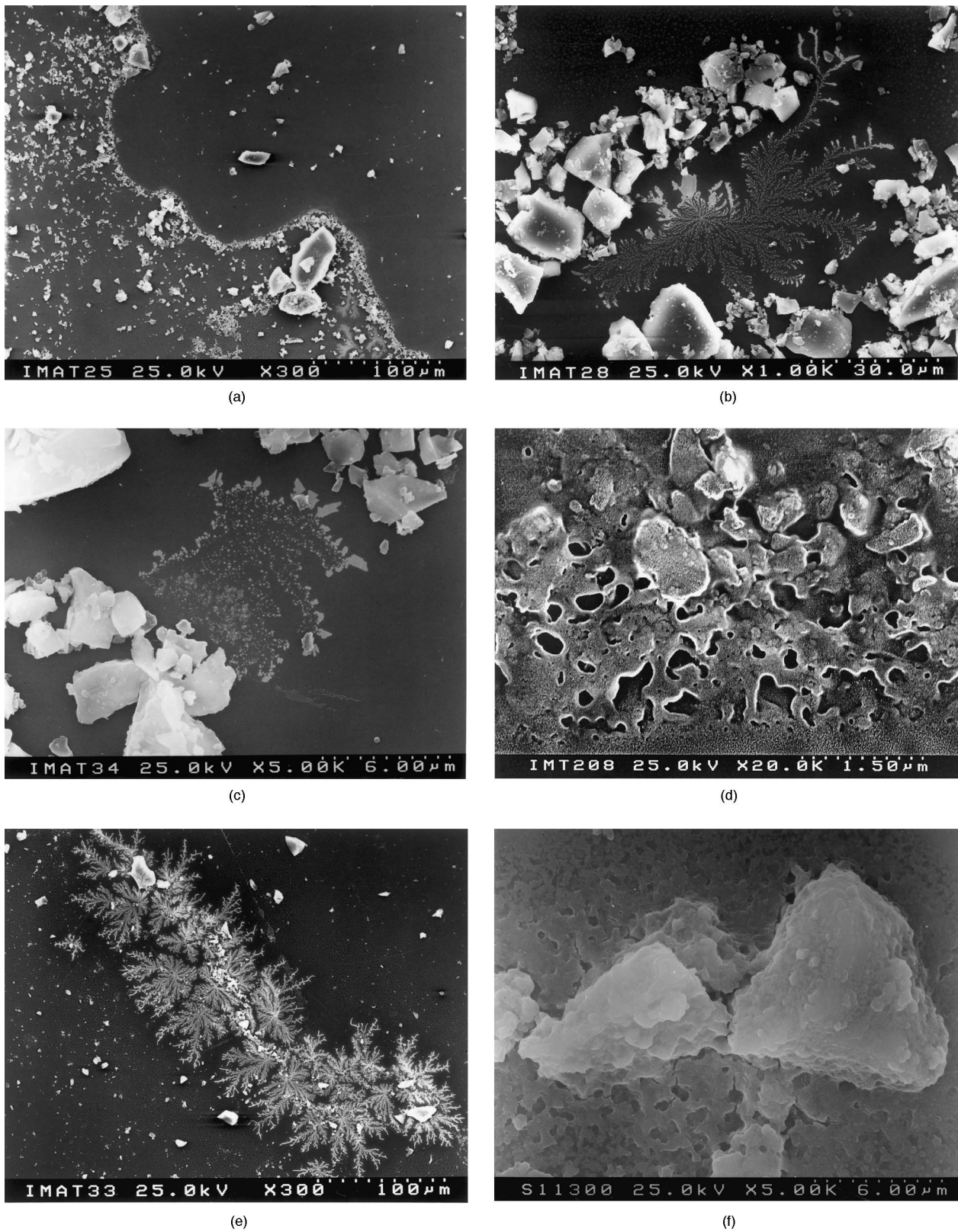
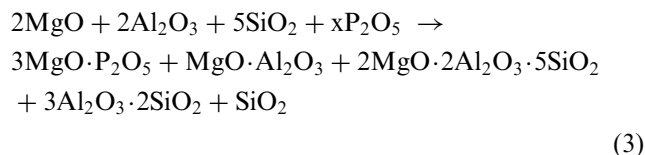


Fig. 3. The morphology of the S series heat-treated at different temperatures for different holding times (a)  $S_0$  950°C/2 h; (b)  $S_1$  950°C/2 h; (c)  $S_6$  950°C/2 h; (d)  $S_1$  1100°C/2 h; (e)  $S_1$  1100°C/2 h; (f)  $S_1$  1300°C/2 h.

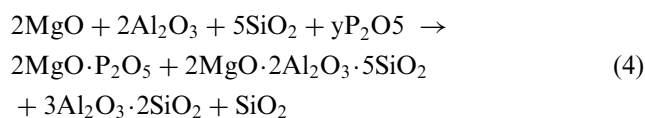
magnesium pyrophosphate at higher concentrations ( $S_4$  to  $S_6$ ). Actually, both magnesium phosphate phases formed seem to play inhibitory roles in the  $\mu \rightarrow \alpha$ -cordierite transition. The amount of farringtonite formed in the sample  $S_1$  was too small and the promoting effect of the additive predominates. The inhibitory effect of the magnesium phosphate phases can be understood since their formation involves the consumption of MgO, driving the composition into the mullite phase field. Amista et al.<sup>11</sup> observed that the formation of  $\alpha$ -cordierite is favoured near stoichiometric cordierite composition, particularly in the MgO-rich region. Therefore, competition by the  $P_2O_5$  additive for the MgO will result in a shortage of this oxide for forming cordierite. The shortage of MgO is still somewhat aggravated due to the formation of traces of spinel phase,  $MgO \cdot Al_2O_3$ .

The complex chemical reactions occurring in the samples in the  $P_2O_5$  additive concentrations range up to 9.74wt%,  $S_4$ , can be described as follows:



As the concentration of the  $P_2O_5$  additive gradually increases from  $S_1$  to  $S_3$ , more MgO would react with  $P_2O_5$  to form farringtonite according to reaction (3). Therefore, cordierite was more difficult to form. This is confirmed by the increased activation energies (Table 2), observed with increasing additive concentrations. As the temperature increases to 1300°C, farringtonite reacts with mullite to form  $\alpha$ -cordierite (Table 1).

When the concentration of  $P_2O_5$  additive further increases from  $S_4$  to  $S_6$ , magnesium pyrophosphate ( $2MgO \cdot P_2O_5$ ) is formed at 1100°C and still persists at 1300°C. The formation of this less MgO rich magnesium phosphate is due to the gradual depletion of MgO in the composition. As a consequence, the corresponding excess amounts of silica and alumina, which initially tend to form solid solutions, will segregate as mullite phase for higher  $P_2O_5$  concentrations. These reactions might be described as follows:



The activation energy reaches a maximum at  $S_4$  (Table 2) where magnesium pyrophosphate starts to appear. This situation should probably correspond to the higher deviation of the remaining composition from the stoichiometric cordierite composition. In fact, the intensity of the magnesium pyrophosphate peaks remains almost constant from  $S_4$  to  $S_5$ , while those of mullite increase. The precipitation of an increasing amount of mullite

would drive the remaining composition towards the stoichiometric composition. Therefore, according to the discussion above, a decrease in the activation energy might be expected, as observed in Table 2. The proportions among the cordierite forming oxides achieved at  $S_5$  will again be changed towards the opposite direction when more  $P_2O_5$  additive was added,  $S_6$ . This might explain why the activation energy tends to increase again.

The results show that there exists a very complicated dynamics balance between the above reactions. However, the reason that at  $S_5$  shows a decreasing value of activation energy is uncertain. Further work is being carried out in order to clarify this point.

From the above analysis, the effect of  $P_2O_5$  on the activation of cordierite can be attributed to the nucleating role-played by  $P_2O_5$  and the formation of  $MgO \cdot P_2O_5$  compounds. At lower  $P_2O_5$  concentrations,  $3MgO \cdot P_2O_5$  was formed, while  $2MgO \cdot P_2O_5$  was formed at higher  $P_2O_5$  concentrations. It can be expected that with further addition of  $P_2O_5$ ,  $MgO \cdot P_2O_5$  will be formed.

## 5. Conclusions

1. The  $P_2O_5$  additive was found to promote the  $\mu$ -cordierite to  $\alpha$ -cordierite transition at lower concentration, while a non-steady inhibitory effect was showed for higher concentrations. This effect could be attributed to the nucleating role played by  $P_2O_5$  and to the formation of mullite and  $xMgO \cdot P_2O_5$  based compounds ( $x = 3, 2, 1$ ).
2. The activation energies with various  $P_2O_5$  additive concentrations as calculated by using Kissinger equation varied from 109 to 701 kJ/mol when the composition changed from  $S_1$  to  $S_4$ , followed by a non-steady evolution for higher concentrations.
3. The degree of conversion from  $\mu \rightarrow \alpha$ -cordierite at 1100°C with 4 h first increases with increasing  $P_2O_5$  additive concentration up to  $S_1$ , decreasing afterwards up to zero for the sample  $S_4$ . Smaller non-steady changes are observed for higher  $P_2O_5$  additive concentrations, which are consistent with the variations in the activation energy.

## Acknowledgements

The first and the second authors are grateful to Fundação Para a Ciência e a Tecnologia of Portugal for the grants.

## References

1. Byung, C. L. and Hyun, M. J., Homogeneous fabrication and densification of cordierite–zirconia composites by a mixed colloidal processing route. *J. Am. Ceram. Soc.*, 1993, **76**(6), 1482–1490.

2. Blodgett, A. J. and Barbour, D. R., Thermal conduction module, a high-performance multilayer ceramic package. *IBM J. Res. Devel.*, 1982, **26**, 30–36.
3. McMillan, P. W. et al., Development of the alpha-cordierite phase in glass-ceramics for use in electronic devices. *Soc. Glass Tech.*, 1985, **6**(26), 286–292.
4. MacDowell, J. F. and Beall, G. H., Low K glass-ceramics for microelectronic packaging. In *Ceramic Transactions*. Vol. 15, The American Ceramic Society, 1990, pp. 259–277.
5. Selvarj, U., Komarneni, S. and Roy, R., Seeding effects on crystallization temperature of cordierite glass powder. *J. Mater. Sci.*, 1991, **26**, 3689–3692.
6. Okuyama, M., Fukui, T. C. and Sakurai, C., Phase transformation and mechanical properties of B<sub>2</sub>O<sub>3</sub>-doped cordierite derived from complex-alkoxide. *J. Mater. Sci.*, 1993, **28**, 4465–4470.
7. Sung, Y. M., The effect of additives on the crystallization and sintering of 2MgO–2Al<sub>2</sub>O<sub>3</sub>–5SiO<sub>2</sub> glass-ceramics. *J. Mater. Sci.*, 1996, **31**, 5421–5427.
8. Sei, T., Eto, K. and Tsuchiya, T., The role of boron in low-temperature synthesis of indialite ( $\alpha$ -Mg<sub>2</sub>Al<sub>4</sub>Si<sub>5</sub>O<sub>18</sub>) by sol–gel process. *J. Mater. Sci.*, 1997, **32**, 3013–3019.
9. Knickerbocker, U., Overview of the glass-ceramic/copper substrate — a high-performance multilayer package for the 1990s. *Am. Ceram. Soc. Bull.*, 1992, **71**(9), 1393–1401.
10. Rudolph, T., Pannhorst, W. and Petzow, G., Determination of activation energies for the crystallisation of a cordierite-type glass. *J. Non-Crys. Solids*, 1993, **155**, 273–281.
11. Amista, P., Cesari, M., Montenero, A., Gnappi, G. and Lan, L., Crystallisation behaviour in the system MgO–Al<sub>2</sub>O<sub>3</sub>–SiO<sub>2</sub>. *J. Non-Crys. Solids*, 1995, **192&193**, 529–533.
12. Suzuki, H., Ota, K. and Saito, H., Preparation of cordierite ceramics from metal-alkoxides, Part 1. *Yogyo Kyokaish*, 1987, **95**(2), 163–169.
13. Ismail, M. G. M. U., Tsunatori, H. and Nakai, Z., Preparation of mullite cordierite powders by the sol–gel method: its characteristics and sintering. *J. Am. Ceram. Soc.*, 1990, **73**(3), 537–543.
14. Okuyama, M., Fukui, T. and Sakurai, C., Effect of complex precursors on alkoxide-derived cordierite powder. *J. Am. Ceram. Soc.*, 1992, **75**(1), 153–160.
15. Spurr, R. A. and Mysers, H., Quantitative analysis of anatase-rutile mixtures with an X-ray diffractometer. *Anal. Chem.*, 1957, **29**, 760–762.
16. Kissinger, H. E., Variation of peak temperature with heating rate in differential thermal analysis. *J. Res. Natl. Bur. Stand*, 1956, **57**, 217–221.
17. Glendenning, M. D. and Lee, W. E., Microstructural development on crystallising hot-pressing pellets of cordierite melt-derived glass containing B<sub>2</sub>O<sub>3</sub> and P<sub>2</sub>O<sub>5</sub>. *J. Am. Ceram. Soc.*, 1996, **79**(3), 705–713.
18. Knickerbocker, S. H., Kumar, A. H. and Herron, L. W., Cordierite glass-ceramics for multilayer ceramic packaging. *Am. Ceram. Soc. Bull.*, 1992, **72**(1), 90–95.
19. Ye, R. I., Fan, Y. H. and Lu, P. W., Glass-ceramics. In *Physics Chemistry of Inorganic Materials*. China constructor industry publication, Beijing, 1984 (in Chinese), pp. 289–290.